Electronic Supporting Information

Selective luminescent sensing of metal ionsand nitro-aromatics over a porous mixed-linker cadmium(II) based metal-organic framework

Rakesh Debnath,[a] Rahul Bhowmick,[a] Pameli Ghosh,[a] Saptarshi Biswas[b] and Subratanath Koner*, [a]

Table S1. Bond distances (Å) and angles (º) around the metal centre in Cd-MOF1

Atoms	**Distance**	**Atoms**	**Distance**
Cd1 - O1	2.241(5)	Cd1 - O4[a]	2.437(6)
Cd1 - O3[a]	2.325(6)	Cd1 - N3	2.368(6)
Cd1 - O2[b]	2.324(6)		
Atoms	**Angle**	**Atoms**	**Angle**
O1 - Cd1 - N3	90.57(10)	O2[b] - Cd1 - N3	86.68(11)
O1 - Cd1 - O3[a]	142.72(18)	N3 - Cd1 - N3[c]	172.32(15)
O1 - Cd1 - O4[a]	88.27(18)	O3[a] - Cd1 - O4[a]	54.45(16)
O1 - Cd1 - O2[b]	128.73(18)	O2[b] - Cd2 - O3[a]	88.56(15)
O3[a] - Cd1 - N3	91.85(10)	O2[b] - Cd2 - O4[a]	143.01(15)
O4[a] - Cd1 - N3	93.82(11)		
Symmetry element [a]= 1-x,-1/2+y,3/2-z; [b]= x,1-y,1-z; [c]= 1-x,y,z			

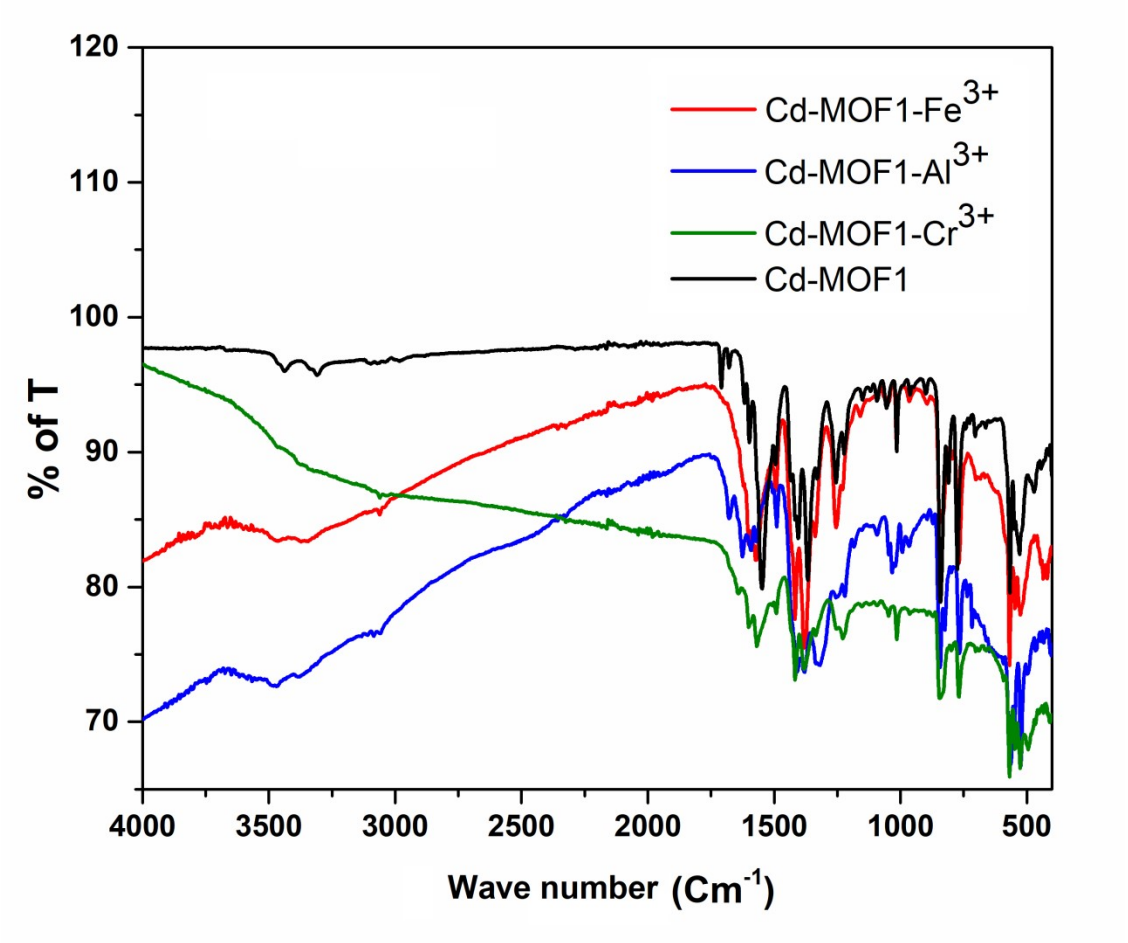

Fig. S1 IR spectra of Cd-MOF1 and Cd-MOF1 treated with various metal salt solutions

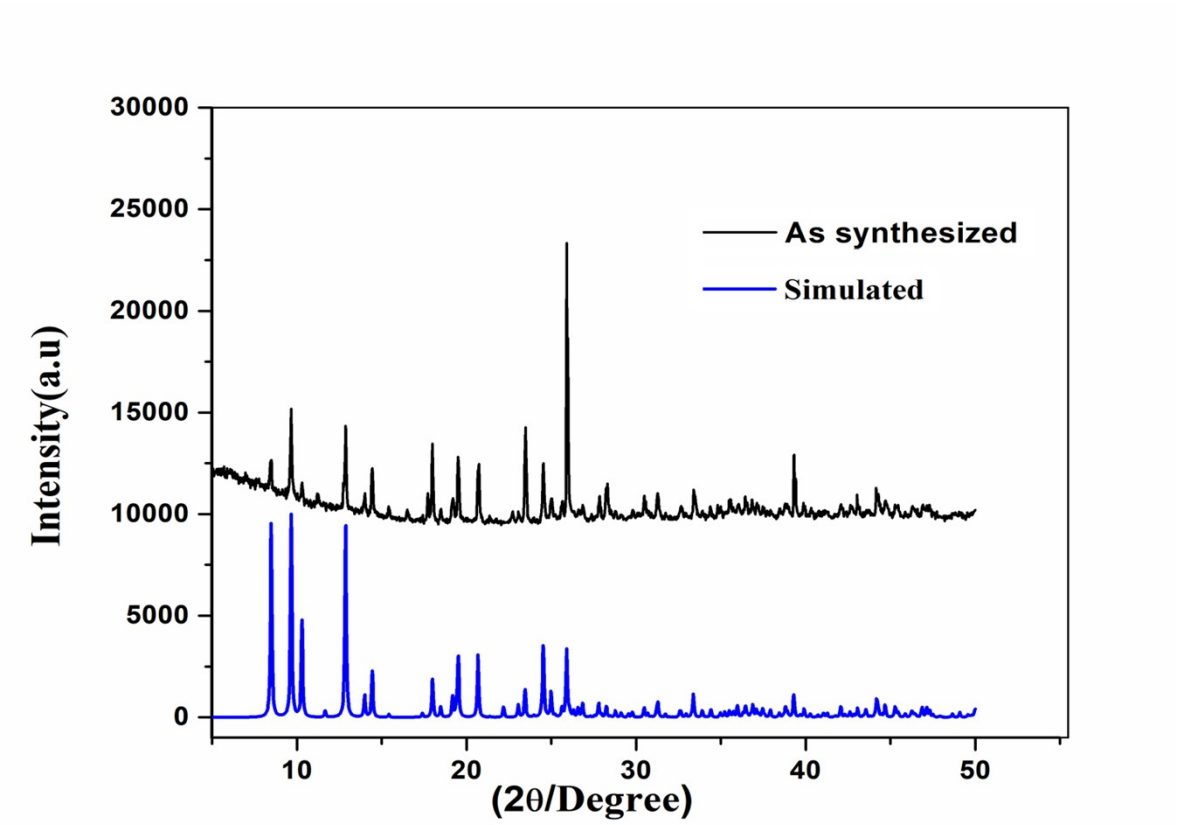

Fig. S2 Powder X-ray diffraction pattern of Cd-MOF1 simulate (blue) and as synthesize (black).

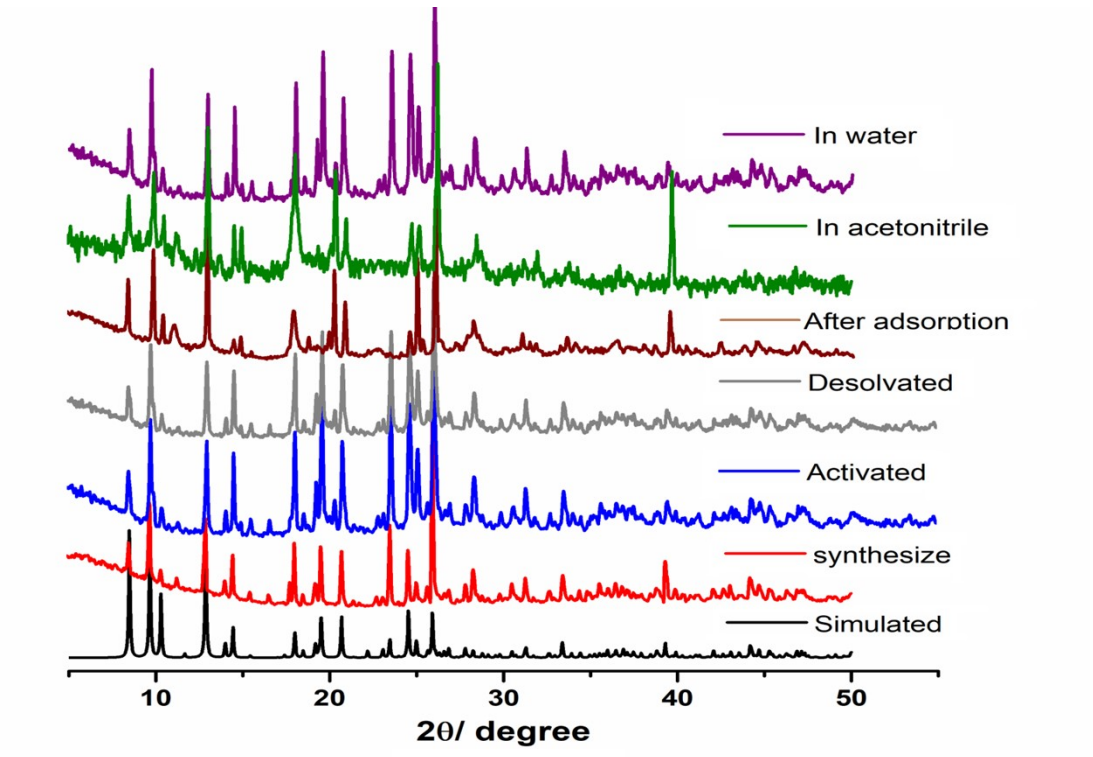

Fig. S3a Powder X-ray diffraction pattern of Cd-MOF1 at different conditions

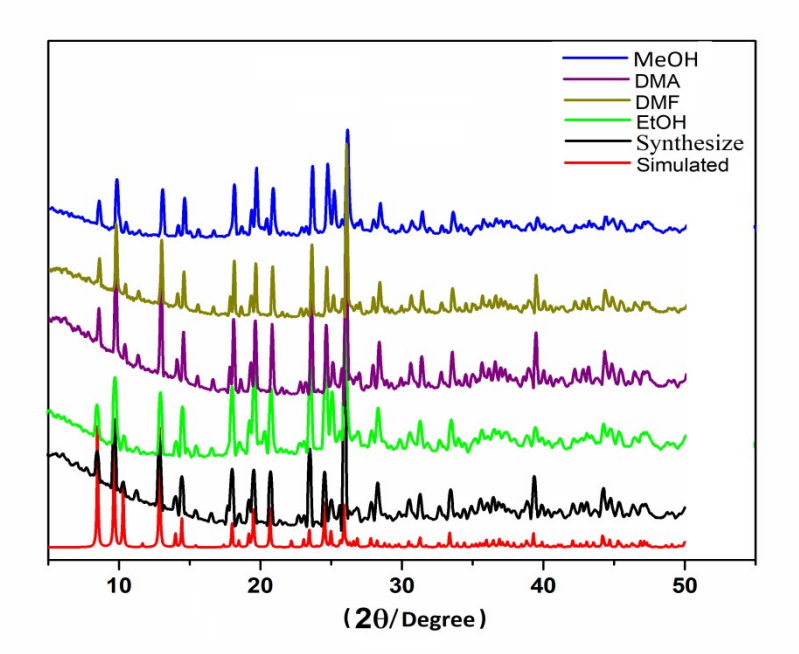

Fig. S3b Powder X-ray diffraction pattern of Cd-MOF1 after immersing in various solvents

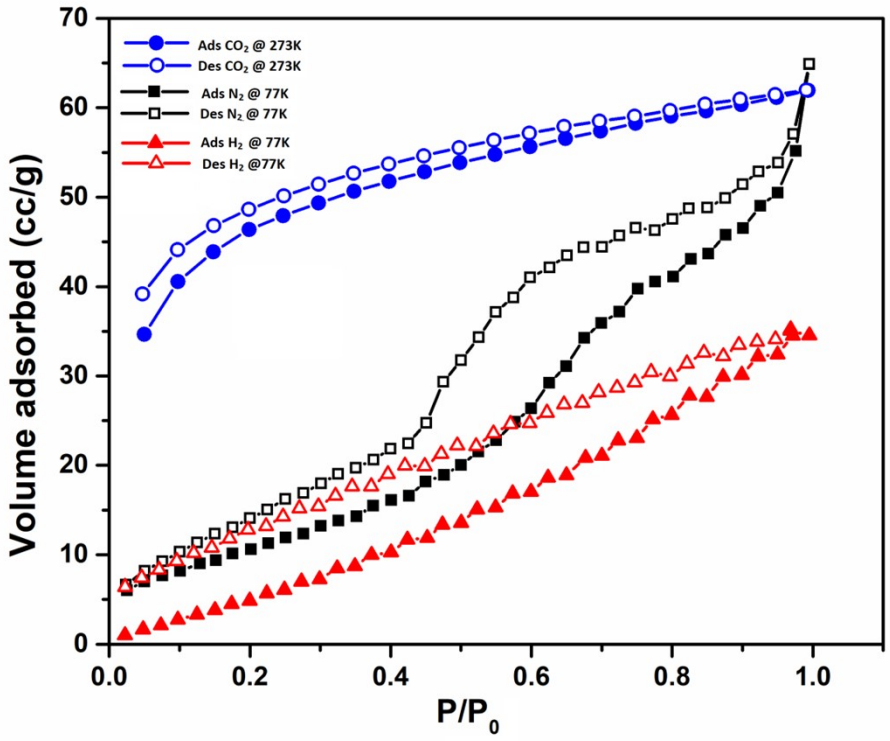

Fig. S4a Gas adsorption isotherms of N_2 (black), H_2 (red) measured at 77K and CO_2 (blue) measured at 273K

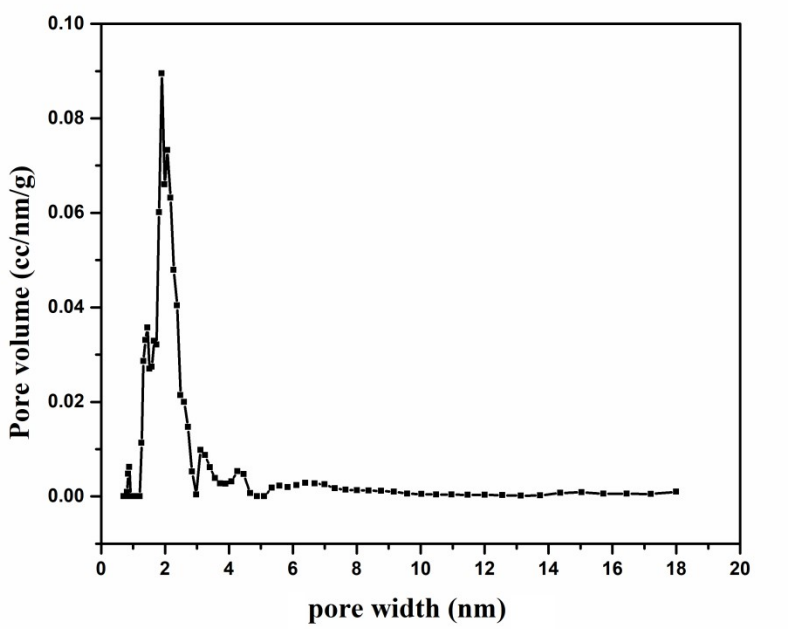

Fig. S4b Pore size distribution plot of Cd-MOF1 calculated using NLDFT method

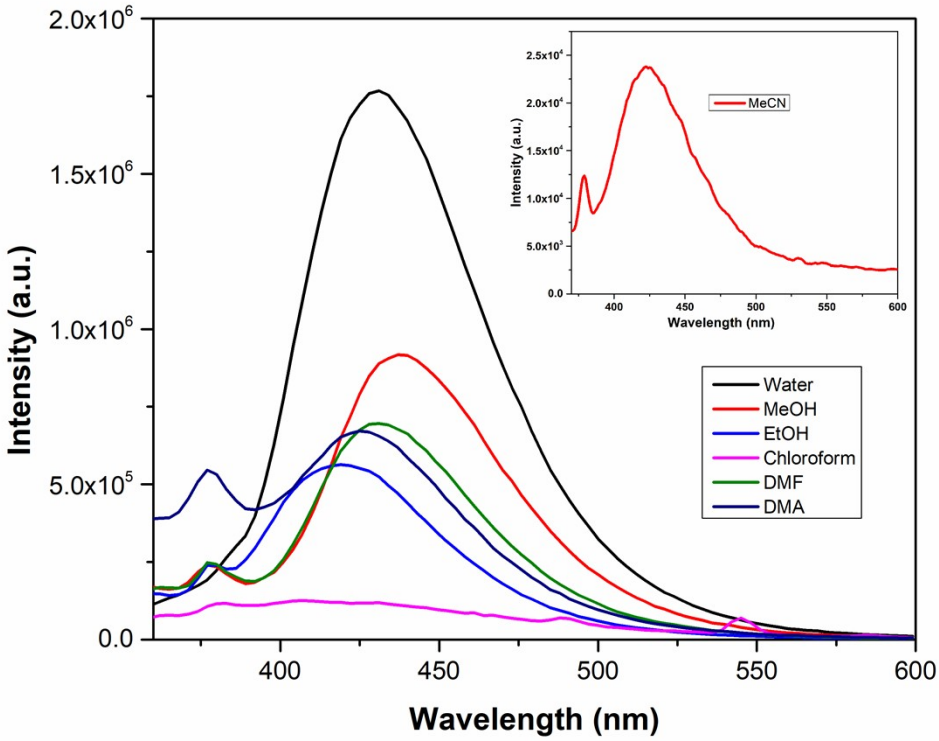

Fig. S5a Comparison of fluorescence spectra of Cd-MOF1 dispersed in various solvent media (λ_{ex}= 370 nm). Fluorescence response of Cd-MOF1 dispersed in MeCN (inset) is weaker than other solvents.

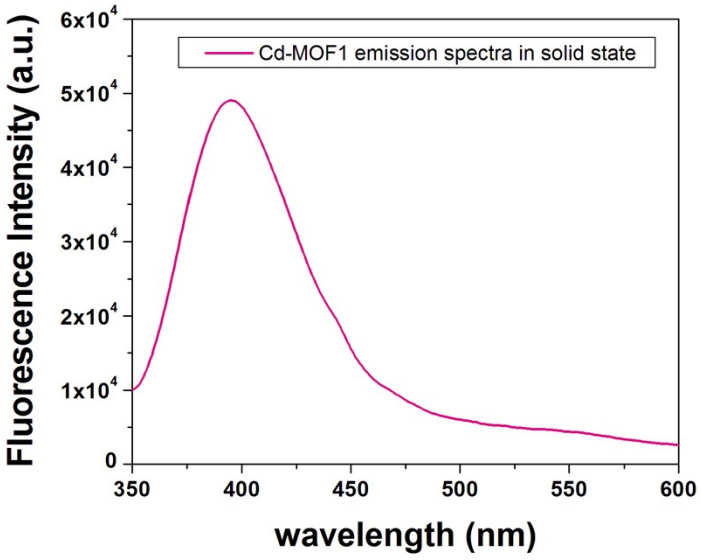

Fig. S5b Solid state emission spectrum of Cd-MOF1 (λ_{ex}= 340 nm).

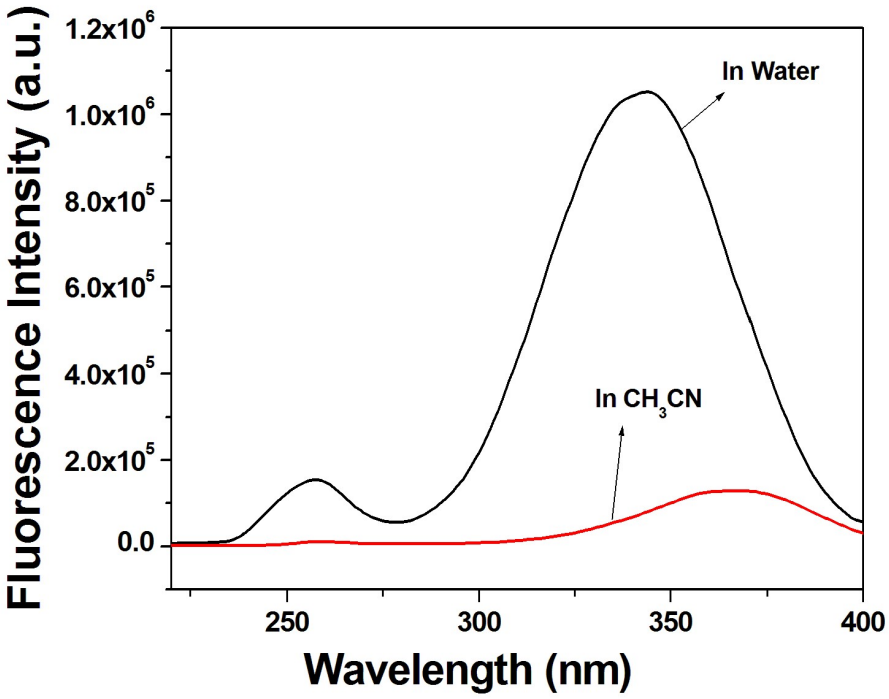

Fig. S5c Comparison of excitation spectrum of Cd-MOF1 (10 μM) at λ_{em} = 428 nm in acetonitrile and water media.

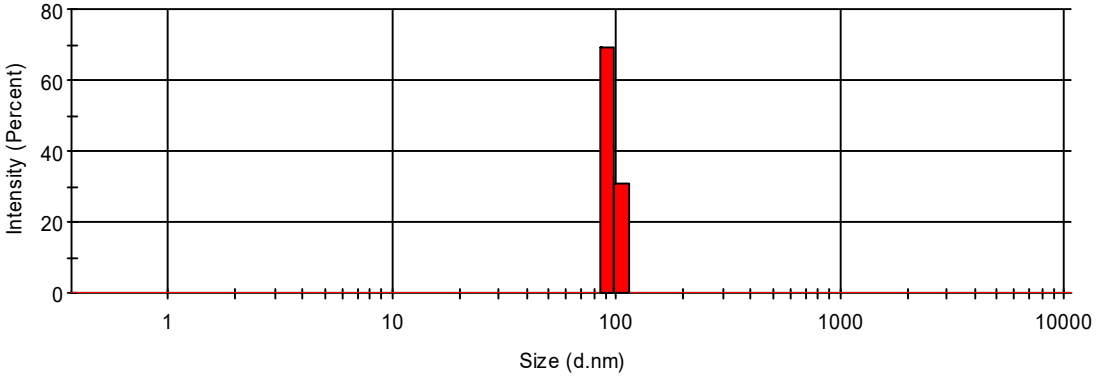

Fig. 6a Dynamic light scattering plot showing particle size distribution of Cd-MOF1 (2 μM) in water medium

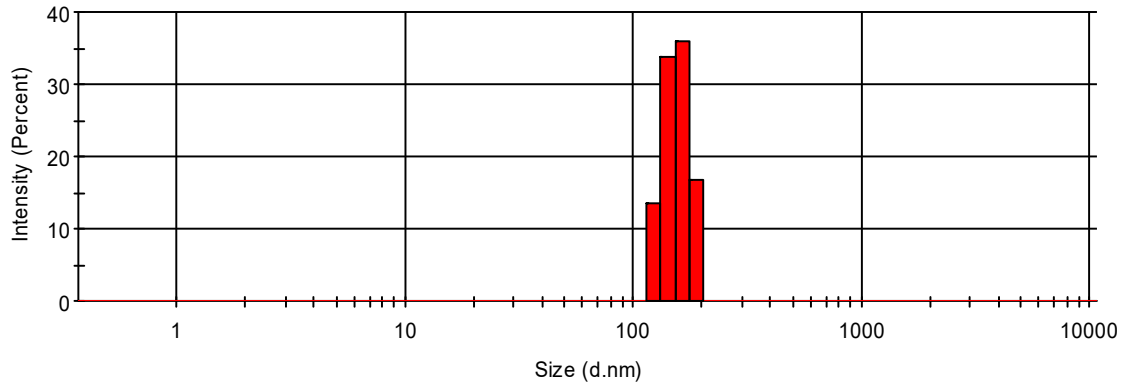

Fig. 6b Dynamic light scattering plot showing particle size distribution of Cd-MOF1 (2 μM) in presence of TNP (2μM) in water medium

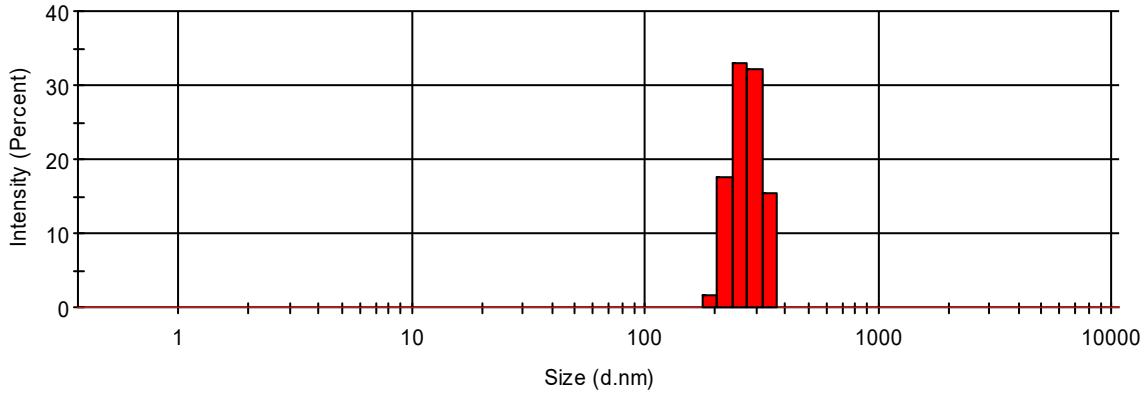

Fig 6c Dynamic light scattering plot showing particle size distribution of Cd-MOF1 (5 μM) in presence of TNP (5μM) in water medium

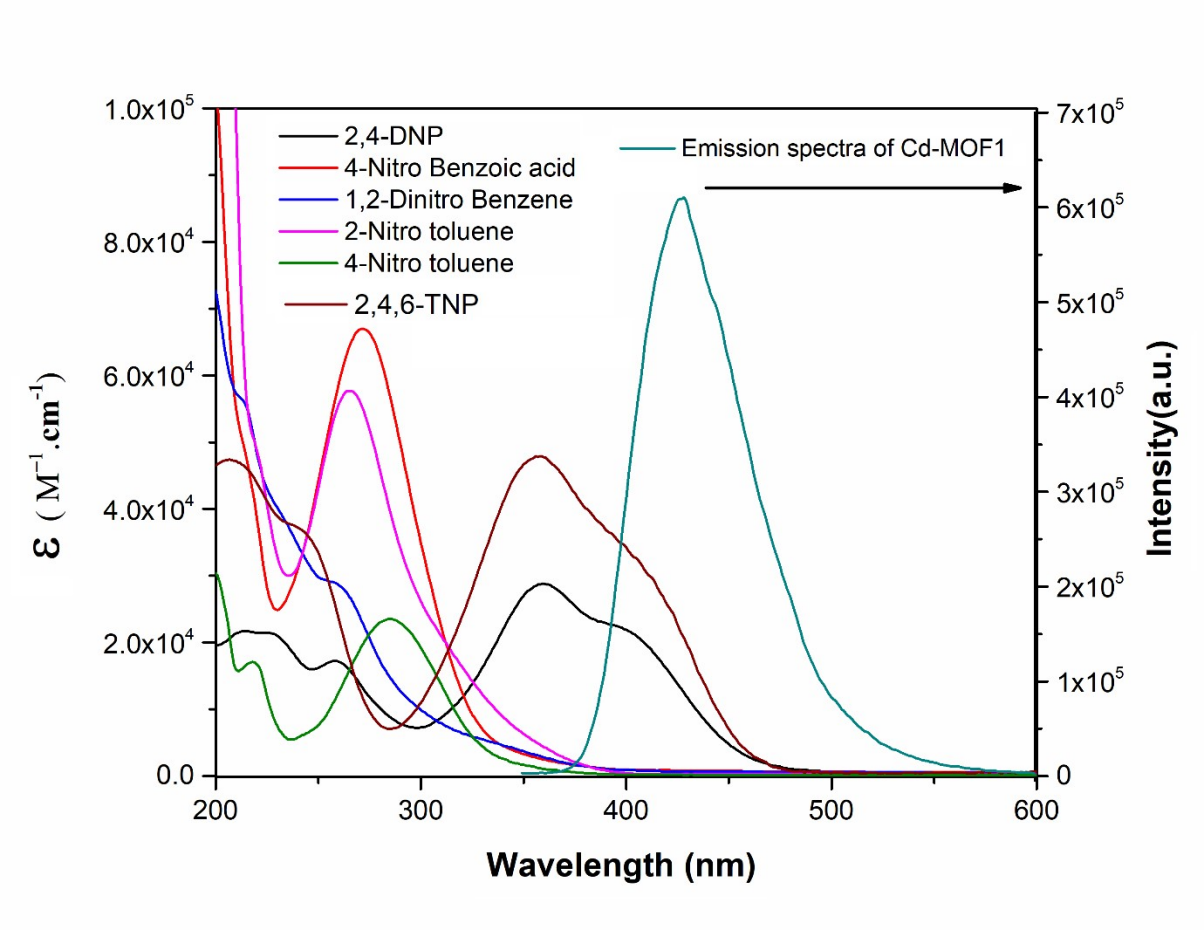

Fig. S7 Plot showing the extent of spectral overlap between absorption band of nitroaromatics and emission band of the Cd-MOF1

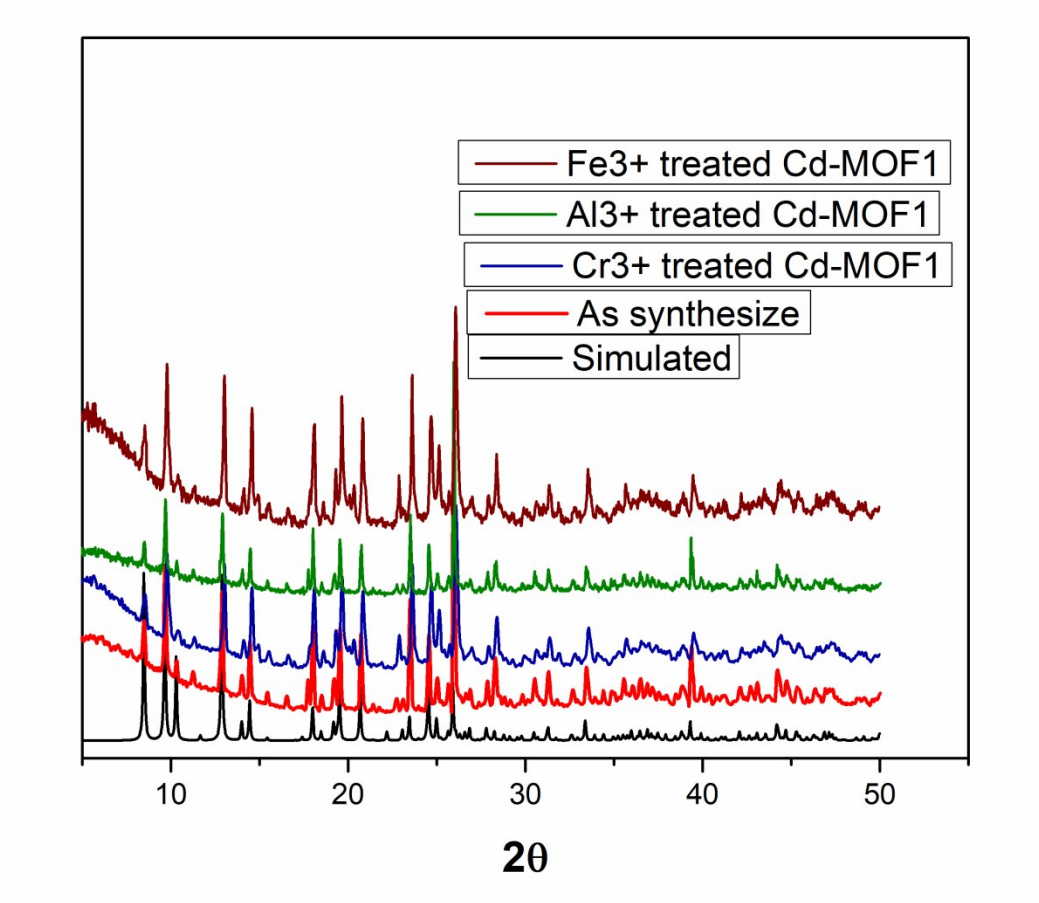

Fig. S8 Powder X-ray diffraction patterns of Cd-MOF1 and solid recovered after metal ion (Fe^{3+}, $Al^{3+}$and Cr^{3+}) sensing experiment

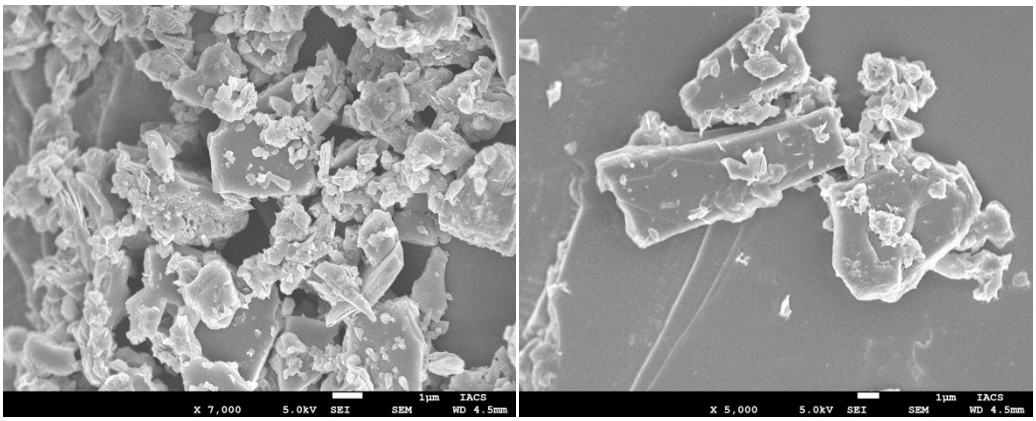

(A) **(B)**

Fig. S9a FE-SEM images of pure Cd-MOF1 (A) and metal treated Cd-MOF1 (B)

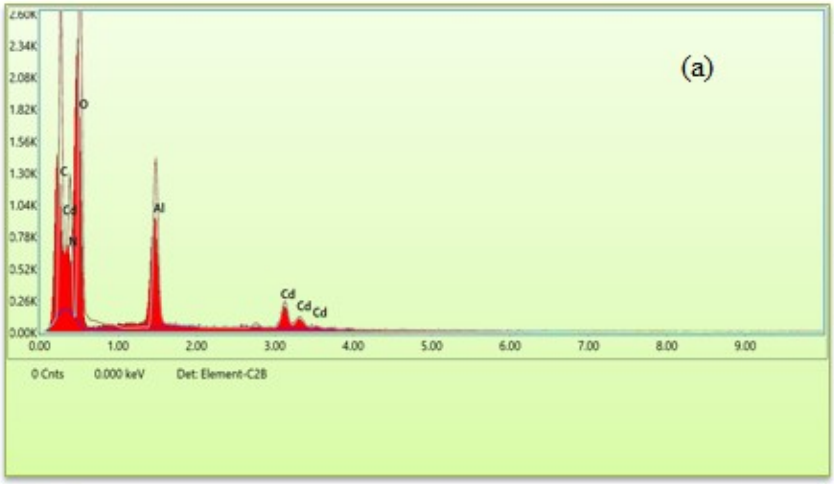

Element	Weight %
C K	25.49
N K	16.89
O K	43.01
AlK	8.69
CdL	5.92

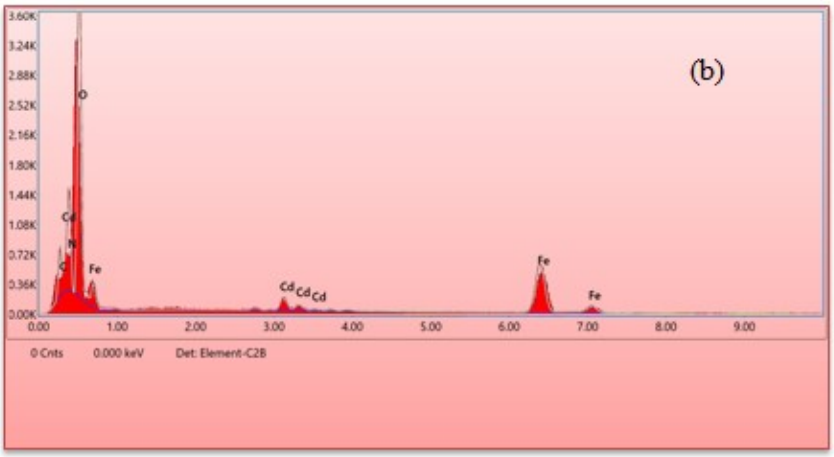

Element	Weight %
C K	7.16
N K	11.15
O K	39.99
CdL	4.68
FeK	37.02

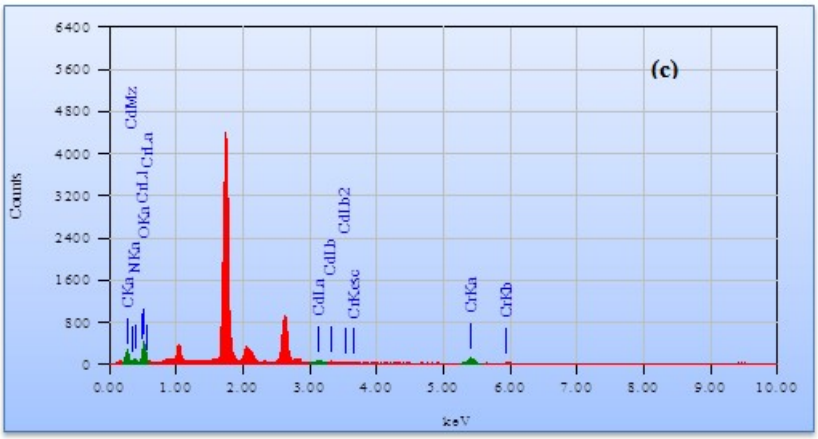

Element	Weight %
C K	12.3528
N K	13.0594
O K	29.3898
CdL	14.3553
CrK	30.8427

Fig. S9b EDS analysis of (a) Al^{3+} treated Cd-MOF1; (b) Fe^{3+} treated Cd-MOF1; (c) Cr^{3+} treated Cd-MOF1.

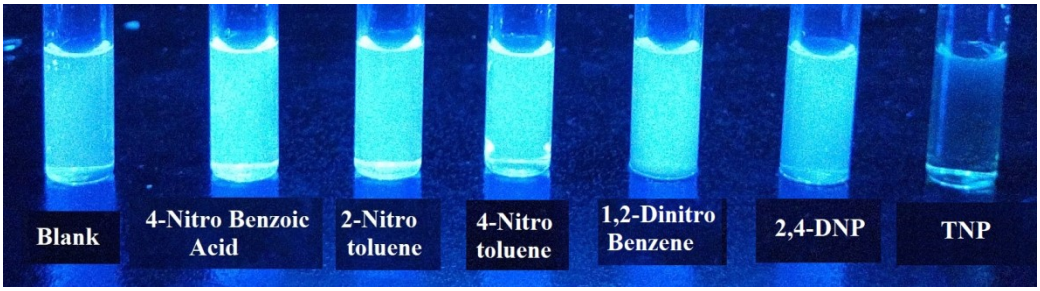

Fig. S10a Visual change of fluorescence intensity of Cd-MOF1 (in water) addition of nitro-explosives under UV light

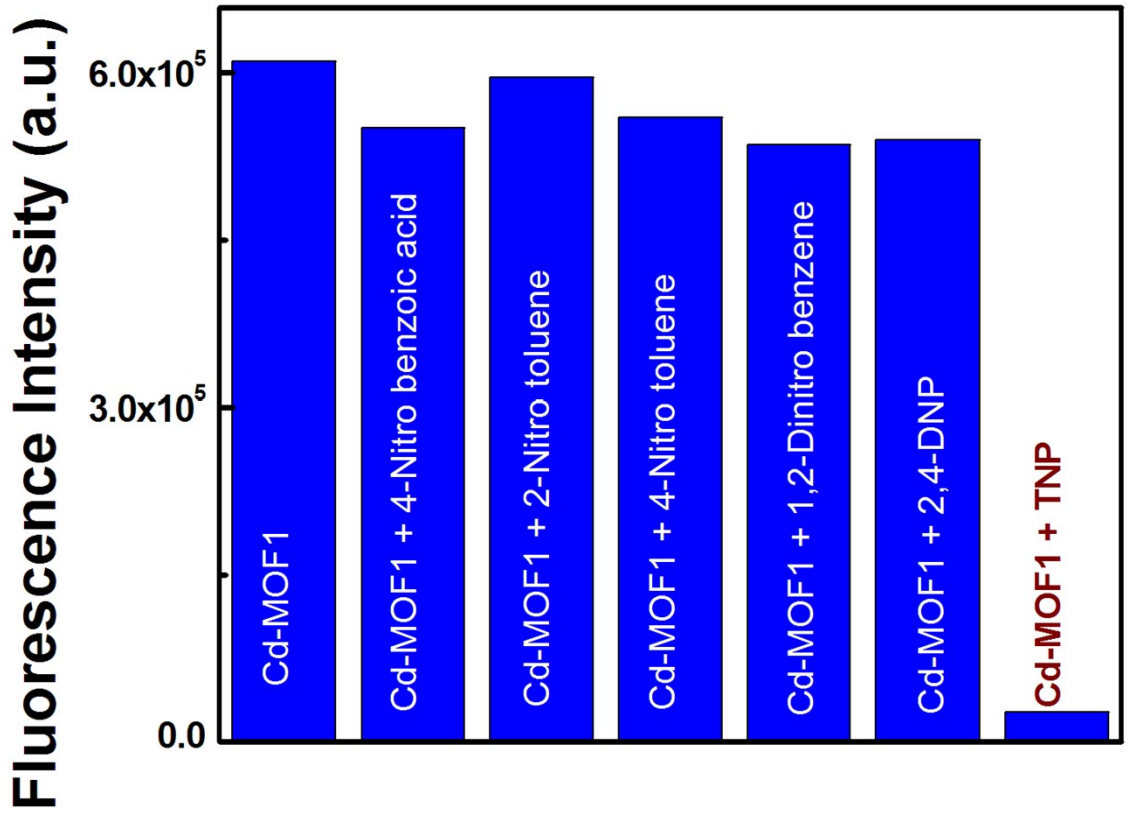

Fig. S10b Bar chart showing fluorescence response of Cd-MOF1 towards different nitroaromatics